Available online at www.sciencedirect.com
SCIENCE DIRECT®
Journal of Molecular Graphics and Modelling 23 (2005) 457–464
Journal of Molecular Graphics and Modelling
www.elsevier.com/locate/JMGM

Modeling aided design of potent glycogen phosphorylase inhibitors

Qiaolin Deng [a,*], Zhijian Lu [b], Joann Bohn [b], Kenneth P. Ellsworth [c], Robert W. Myers [c], Wayne M. Geissler [c], Georgianna Harris [c], Christopher A. Willoughby [b], Kevin Chapman [b], Brian McKeever [d], Ralph Mosley [a]

[a] *Department of Molecular Systems, Merck Research Laboratories, Merck & Co. Inc., P.O. Box 2000, Rahway, NJ 07065, USA*
[b] *Department of Medicinal Chemistry, Merck Research Laboratories, Merck & Co. Inc., P.O. Box 2000, Rahway, NJ 07065, USA*
[c] *Department of Metabolic Disorders, Merck Research Laboratories, Merck & Co. Inc., P.O. Box 2000, Rahway, NJ 07065, USA*
[d] *Department of Structural Biology, Merck Research Laboratories, Merck & Co. Inc., P.O. Box 2000, Rahway, NJ 07065, USA*

Received 6 December 2004; received in revised form 5 January 2005; accepted 6 January 2005

Abstract

Molecular modeling has been used to assist in the development of a novel series of potent glycogen phosphorylase inhibitors based on a phenyl diacid lead, compound 1. In the absence of suitable competitive binding assays, compound 1 was predicted to bind at the AMP allosteric site based on superposition onto known inhibitors which bind at different sites in the enzyme and analyses of the surrounding protein environment associated with these distinct sites. Possible docking modes of compound 1 at the AMP allosteric site were further explored using the crystal structure of rabbit muscle glycogen phosphorylase complexed with a Bayer diacid compound W1807 (PDB entry 3AMV). Compound 1 was predicted to interact with positively charged arginines at the AMP allosteric site in the docking model. Characterization of the binding pocket by a grid-based surface calculation of the docking model revealed a large unfilled hydrophobic region near the central phenyl ring, suggesting that compounds with larger hydrophobic groups in this region would improve binding. A series of naphthyl diacid compounds were designed and synthesized to access this hydrophobic cleft, and showed significantly improved potency

Keywords: Glycogen phosphorylase (GP); AMP allosteric site; Diacid inhibitors; Superposition; Docking

1. Introduction

It is estimated that over 100 million people worldwide are affected by type 2 diabetes [1], which, left untreated, can lead to serious complications such as nerve damage, kidney failure, blindness and cardiovascular diseases [2]. Type 2 diabetes is a chronic metabolic disorder characterized by fed and fasting hyperglycemia. Glycogen phosphorylase (GP) is a key enzyme in the regulation of glycogen metabolism, catalyzing the breakdown of glycogen to glucose-1-phosphate. In muscle, glucose-1-phosphate is used to generate metabolic energy, while in liver it is also converted to glucose for export to peripheral tissues. In humans, there are three isozymes of GP named to denote the tissues in which they are predominantly expressed: liver, muscle and brain. The muscle and brain isozymes serve the tissues in which they are found, while the liver isozyme meets the glycemic demands of the body as a whole. Previous reports have indicated that GP inhibition can lower blood glucose in diabetic models, thus, validating it as a potential therapeutic target for treatment of type 2 diabetes [3–5]. However, since inhibition of muscle or brain GP could lead to undesirable side effects, the liver isozyme of human glycogen phosphorylase (HLGP) may be the preferred target for therapeutic intervention with GP inhibitors.

Abbreviations: CP320626, 5-chloro-1H-indole-2-carboxylic acid (1-(4-flurobenzyl)-2-(4-hydroxypiperidin-1-yl)-2-oxoethyl)amide; GP, glycogen phosphorylase; GPa, glycogen phosphorylase a; GPb, glycogen phosphorylase b; HLGP, human liver glycogen phosphorylase; HMGP, human muscle glycogen phosphorylase; ICM, Internal Coordinate Mechanics; PDB, Protein Data Bank; RMGP, rabbit muscle glycogen phosphorylase; W1807, (−)(S)-3-isopropyl 4-(2-chlorophenyl)-1,4-dihydro-1-ethyl-2-methyl-pyridine-3,5,6-tricarboxylate

* Corresponding author. Tel.: +1 732 594 0618; fax: +1 732 594 4224.
E-mail address: qiaolin_deng@merck.com (Q. Deng).

1093-3263/$ – see front matter © 2005 Elsevier Inc. All rights reserved.
doi:10.1016/j.jmgm.2005.01.001

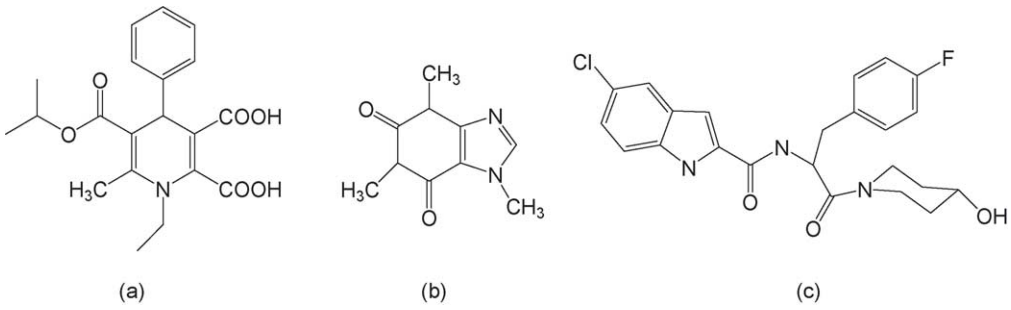

Fig. 1. Examples of known GP inhibitors. (a) Bayer diacid compound W1807 that binds at the AMP allosteric site (PDB entry 3AMV). (b) Caffeine that binds at the inhibitor site (PDB entry 1GFZ). (c) CP320626 that binds at the dimer interface site (PDB entry 1C50).

Human liver glycogen phosphorylase and human muscle glycogen phosphorylase (HMGP) are homodimers with more than 800 amino acid residues in each monomer. GP exists in two inter-convertible forms: a Ser14-phosphorylated high activity form (GPa) and an unphosphorylated low activity form (GPb). Both forms exist in equilibrium between two different conformational states: a more active R-state and a less active T-state [6]. The more active R-state is induced by the substrate and by allosteric effectors such as AMP or IMP, while the less active T-state is stabilized by inhibitor binding. X-ray crystallographic studies of inactive and active conformations of HLGPa demonstrated large conformational changes between the two conformational states, including order/disorder transitions and changes in secondary structure [7]. The inactive conformation of GP was used as the target for inhibitor design and optimization.

GP contains at least six potential regulatory sites: (1) The Ser14-phosphate recognition site; Ser14 phosphorylation induces conformational changes that alter GP activity. (2) The catalytic site, which binds the substrates glycogen and glucose-1-P, as well as glucose and glucose analogues. (3) The AMP allosteric site, which binds AMP, IMP, ATP and glucose-6-P. This site is about 35 Å away from the catalytic site. Bayer diacid W1807 (Fig. 1a), a potent inhibitor of RMGPb (Ki = 1.6 nM), binds at this site as determined by crystallographic analysis [8,9]. (4) The inhibitor site (also referred to as the purine nucleoside site), which binds heterocyclic compounds such as caffeine (Fig. 1b) and flavopiridol. This site is more than 10Å away from the catalytic site [10]. (5) The glycogen storage site. (6) The dimer interface site, which binds indole derivative CP320626 (Fig. 1c) and its analogs [11]. This site was recently identified as a new allosteric site by X-ray crystallographic analysis [12–14]. Four of these six regulatory sites are known to be inhibitor binding sites: the catalytic site, the AMP allosteric site, the inhibition site and the dimer interface site.

In this paper, the use of molecular modeling in the development of a series of potent GP inhibitors is described. One of the lead series is composed of phenyl diacids with various substitutions on the pyridine (Fig. 2a). Of these, the most potent compound is 4(2-(((4-nitropyridine-2 yl)carbonyl)amino)phenoxy)phthalic acid (compound 1). Due to the lack of competitive binding studies, modeling studies were undertaken to ascertain the most probable binding site for compound 1. These involved superposition [15] onto known

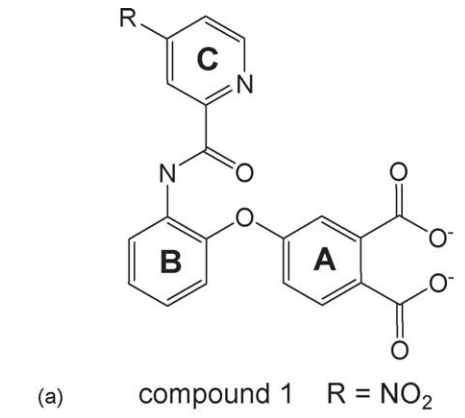

Fig. 2. Lead compound 1 and its lowest-energy conformation. (a) Chemical structure of lead compound series. (b) The lowest-energy conformation of compound 1 from gas phase calculations. The molecule is shown in stick with carbons in green and non-carbon atoms in standard colors.

inhibitors, which bind at different sites in the enzyme, as well as examination of the protein environment to determine the possibility of interaction with nearby residues. Ultimately, these analyses suggested that compound 1 binds at the AMP allosteric site. The docking of compound 1 inside the AMP allosteric site was further explored by ICM calculations [16] with subsequent energy minimization. Additional characterization of the binding pocket by grid-based surface calculations [17] revealed a large unfilled hydrophobic region near the central phenyl ring which provided an opportunity to potentially enhance binding of early leads by increasing the hydrophobic bulk in this region. A series of naphthyl compounds were designed and synthesized, and demonstrated to display a significant improvement in potency.

2. Methods

2.1. Superposition

Two hundred conformers of compound 1 were generated using our implementation of the distance geometry approach, which incorporates the theory and algorithm as previously described [18]. The conformer set was energy minimized using a distance-dependent dielectric of $2r$ with the MMFFs force field [19–25]. SQ [15] calculations were employed to superpose these conformers onto probes derived from publicly available crystal structures of known inhibitors in complex with GP: W1807 at the AMP allosteric site (PDB entry 3AMV [8]), caffeine at the inhibitor site (PDB entry 1GFZ [10]) and CP320626 at the dimer interface site (PDB entry1C50 [12]). Each probe represents a class of inhibitors at a different binding site and their structures are shown in Fig. 1.

2.2. Docking

Having identified the AMP allosteric site as the most likely binding site for compound 1 through the SQ overlay, a more extensive docking study was carried out using ICM software [16]. The amino acid sequences of HLGP, HMGP and RMGP were aligned using CLUSTAL W [26]; the three isozymes are highly homologous. Due to the lack of a crystal structure of HLGP complexed with an inhibitor at the AMP allosteric site, the high resolution (2.1 Å) crystal structure 3AMV (RMGPa complexed with W1807 [8]) was used as the template for docking. Ligand and water molecules in the crystal structure were removed. The dimer was constructed based on crystallographic symmetry operations, since the AMP allosteric site is formed by residues from both monomers. In the following context, regular residue numbers will be used to describe residues from the first monomer, and residue number with a prime ($'$) will be used to denote residues from the symmetry-related unit. Since the complete dimer consists of more than 1600 amino acids, a smaller enzyme site was created for docking calculations. Residues with any atom falling within a 15 Å shell around W1807 were retrieved to construct the enzyme site.

One hundred initial docking poses within the AMP allosteric site were generated by the ICM [16] calculations. Each of the resultant complexes was then energy optimized using the MMFFs force field [19–25]. In these calculations, the ligand was fully optimized inside the binding pocket, which allowed limited flexibility. The sidechains of residues with any atom located within 5 Å of the ligand were fully minimized in conjunction with the ligand. Residues falling within 5–10 Å of the ligands were included in the calculations as rigid elements and residues beyond a 10 Å cutoff from the ligand were ignored in the calculations. The total energy of the complex, the individual energies of the ligand and the enzyme, and the interaction energy between the ligand and the enzyme were calculated. The best docking mode was determined by selecting those poses with the most stabilizing interaction energy and minimal amount of strain on the ligand and by visual inspection of the interactions.

2.3. Characterization of the binding pocket

The grid generated for FLOG [17] studies was visualized as a series of iso-energetic surfaces to characterize the binding pocket by its polar (hydrogen bond donor and acceptor) and hydrophobic nature as well as its van der Waal limits. Analysis of this enzyme binding site indicated an unexplored region of hydrophobicity near the central phenyl ring of compound 1 in its energetically preferred pose within the AMP allosteric site.

2.4. Energy evaluation of designed compounds

The docking model of lead compound 1 was used as a reference and starting point. The designed compounds were obtained by modifying compound 1 and fully optimized inside the flexible binding pocket, as described above.

2.5. Chemistry

The synthesis route of naphthyl compounds has been previously described by Lu et al. [27].

2.6. Biology

Phosphorolysis of glycogen was carried out using baculovirus expressed, recombinant HLGPa and HMGPa. Glucose-1-phosphate production was monitored via a continuous coupled enzyme assay employing phosphoglucomutase/glucose-6-phosphate dehydrogenase for spectrofluorometric detection of NAD(P)H produced.

3. Results and discussion

3.1. Prediction of putative binding pocket

The lead compounds are a series of phenyl diacids with various substituents on the pyridine (Fig. 2a), the most potent of which incorporates a nitro group onto the pyridine (compound 1). It has an IC_{50} of 3 nM for HLGPa and 25 nM for HMGPa (Table 1). Of the 200 conformers generated and energy minimized, the energetically favored conformation of compound 1 was found to be in a "V" shape (Fig. 2b). In this conformation, the NH group of the amide interacts with the nitrogen atom in the pyridine, perhaps in hydrogen bonding fashion, to stabilize the molecule. The two aromatic rings at the distal ends of the molecule are nearly perpendicular to each other with an edge-to-face distance of about 4 Å, indicating a potentially favorable π–π stacking interaction within the molecule.

Competitive binding studies were not available to aid in the identification of the binding site of these inhibitors. Before detailed docking studies could proceed, it was therefore necessary to first identify the most likely binding site of compound 1. To this end, 3D similarities between conformers of compound 1 and three probes derived from known crystal structures were assessed. The glucose analogue, which acts as an inhibitor at the catalytic site, was dismissed from consideration because of the obvious lack of similarity between it and compound 1. Conformers of compound 1 were compared to the crystal structures of Bayer diacid W1807 at the AMP allosteric site (PDB entry 3AMV [8]), caffeine at the inhibitor site (PDB entry 1GFZ [10]) and Pfizer compound CP320626 at the dimer interface site (PDB entry1C50 [12]), using the 3D similarity/ superposition tool SQ [15]. The best overlay of compound 1 onto each of the three probes is depicted in Fig. 3. Compound 1 overlays onto W1807 (Fig. 3a) with the aromatic regions and diacid groups fairly well aligned. W1807 is most similar to compound 1 among the three probes, so this is not an unexpected result. Like W1807, the diacid moiety of compound 1 presumably interacts with positively charged arginines at the AMP allosteric site. In contrast, the energetically preferred "V" shape of compound 1 precludes it from being able to align well onto the planar structure of caffeine (Fig. 3b). While the superposition of compound 1 onto CP320626 (Fig. 3c) is visually appealing, it requires compound 1 to adopt a conformation energetically disfavored by more than 10 kcal/mol. In this

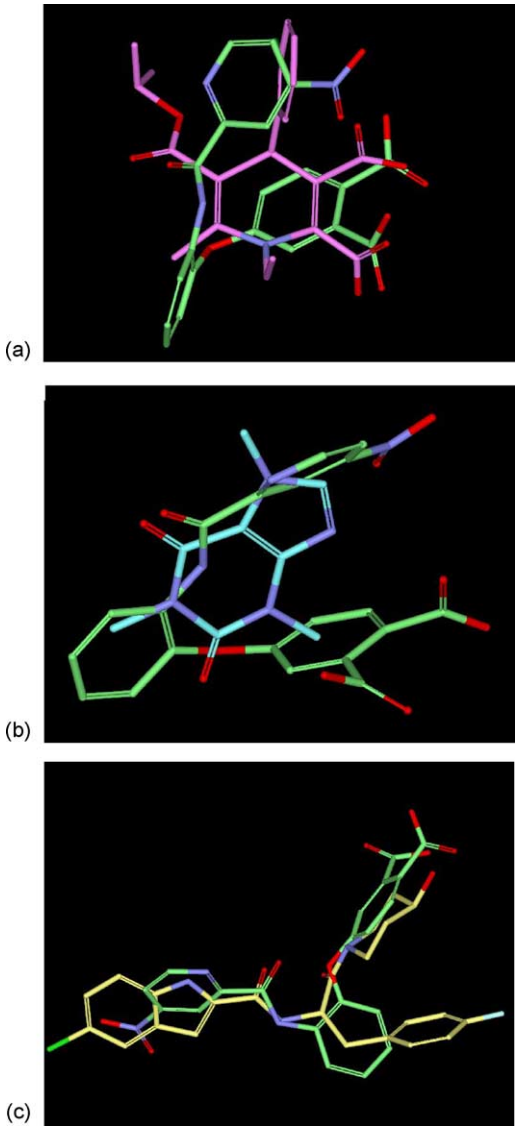

Fig. 3. Superposition of compound 1 onto known inhibitors by SQ calculations. Compound 1 (carbons in green) overlaid onto (a) W1807 (carbons in purple) at the AMP allosteric site, (b) Caffeine (carbons in cyan) at the inhibitor site, (c) CP320626 (carbons in yellow) at the dimer interface site. Only heavy atoms are shown and non-carbon atoms are in standard colors.

Table 1
Comparison of activity of naphthyl and phenyl diacid compounds

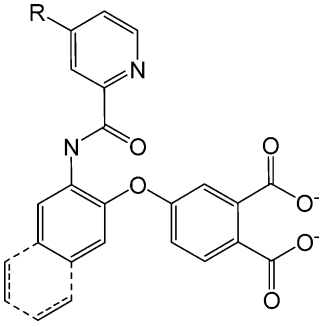

R	HLGPa (IC_{50} nM)		HMGPa (IC_{50} nM)	
	Phenyl	Naphthyl	Phenyl	Naphthyl
$-NO_2$	3	1	25	3
–Cl	17	2	181	12
–OMe	20	2	200	12
$-CF_3$	48	12	591	80
–Et	56	4	433	29
–Me	121	10	1090	57
–H	1280	167	11790	844

alignment, the diacid groups and the A ring are overlapped onto the 4-hydroxy-piperidyl moiety of CP320626, known to bind in a space filled with water molecules at the dimer interface site [12]. As a result, the diacid group in compound 1 cannot make significant favorable interactions with the enzyme. Based on this analysis of each binding site, it appeared likely that compound 1 binds at the AMP allosteric site. This prediction was subsequently confirmed by our X-ray crystal structure of RMGPb complexed with compound 1 [27,28].

3.2. Docking model

HLGP is highly homologous to HMGP and RMGP, with a sequence identity of 80% and similarity of 90%. The homology between HMGP and RMGP is even higher, with a sequence identity of 97% and similarity of 99%. The residues located within 5 Å of W1807 in the AMP allosteric site are conserved among the three isozymes, so it is likely that the binding pocket would be similar amongst them. Due to the lack of a crystal structure of HLGP complexed with an inhibitor bound in the AMP allosteric site, the crystal structures of RMGP complexed with W1807 were used as the templates. Two crystal structures were available for W1807 complexed with RMGP, one in phosphorylated form GPa (PDB entry 3AMV) and one in unphosphorylated form GPb (PDB entry 2AMV) [8,9]. Both crystal structures are in the less active T-state and are structurally similar with a RMSD for the main-chain atoms of ∼0.3 Å [8]. Interactions between W1807 and the residues of the AMP allosteric site are essentially identical in the two structures. The most recent crystal structure of T-state GPa complexed with W1807 at high resolution (2.1 Å) (PDB entry 3AMV [8]) was selected for use in the docking calculations.

The first docking pose of compound 1 at the AMP allosteric site was taken from the superposition onto W1807. Ultimately, this pose proved unsuitable as a starting point for further energy minimization and analysis. This was due, in part, to the lack of any consideration of the nearby protein environment in the superposition calculations.

Instead, ICM [16] calculations were carried out to generate initial docking poses to sample various conformations and locations for compound 1 inside the AMP allosteric binding pocket. The initial docking modes were then energy minimized with compound 1 fully optimized inside the flexible binding pocket. The pose with the most favorable interaction energy and least amount of internal strain on the ligand was determined as a preferred docking mode, as shown in Fig. 4.

The putative binding pocket for compound 1 is formed by helix 2 (residues 47–78), helix 8 (residues 289–314), β sheet 4 (residues 153–160), β sheet 11 (residues 237–247), a short β sheet 7 (residues 191–193) and cap region (residues 36′–47′) from the symmetry-related unit. The ligand maintained the energetically preferred ‘‘V’’ shape with the A and C rings buried inside the AMP allosteric site and the B ring located at the entrance to the binding site. The diacid group of the A ring interacts with three arginines, Arg81, Arg309 and

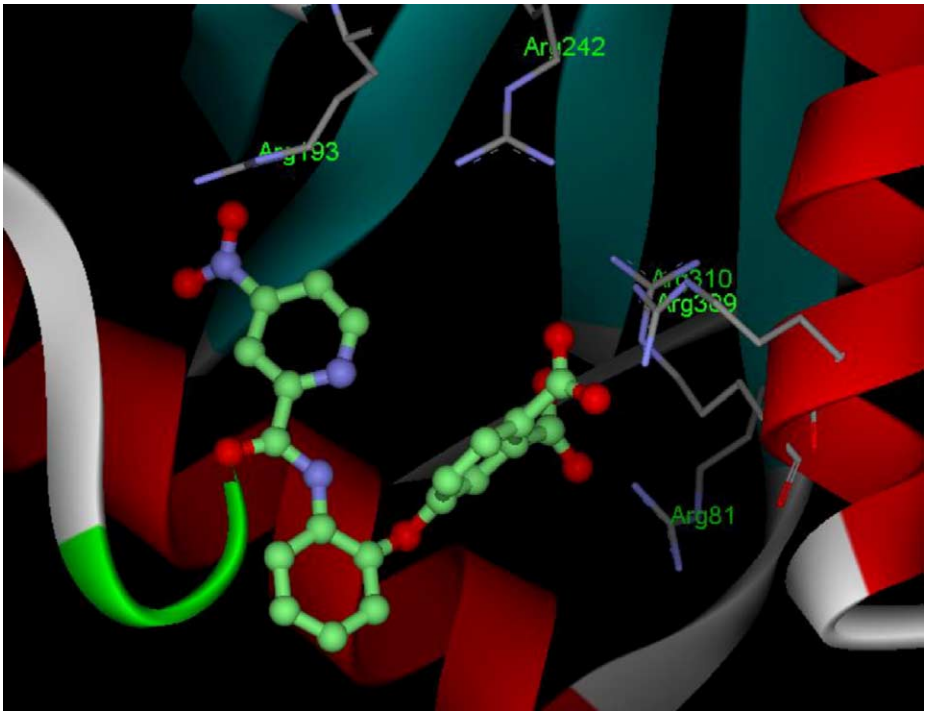

Fig. 4. Docking model of compound 1 inside the AMP allosteric site. The heavy atoms of compound 1 are shown in ball and stick, with carbons in green and non-carbon atoms in standard colors. The GP structure is shown in solid ribbon with helices in red and β-sheets in cyan. Several important arginines in the binding pocket are shown in stick with standard colors. Hydrogen atoms have been omitted for clarity.

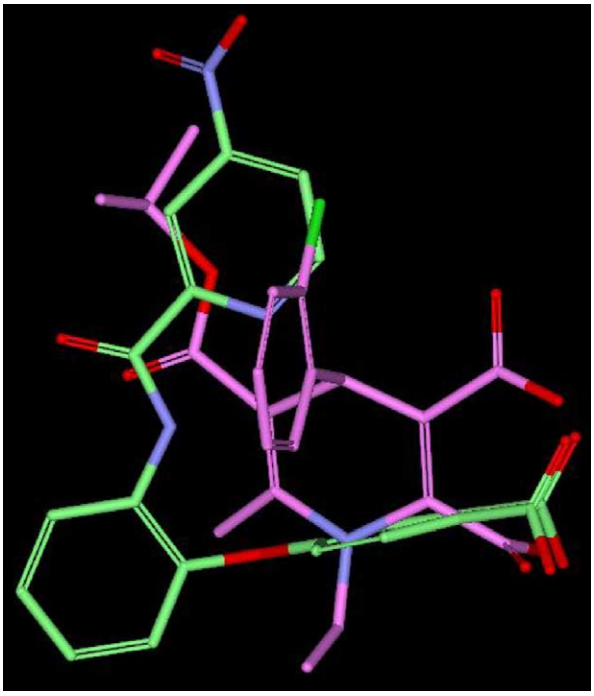

Fig. 5. Comparison of docked compound 1 with crystal structure of W1807. Compound 1 (carbons in green) and W1807 (carbons in purple, PDB entry 3AMV) are shown in stick with non-carbon atoms in standard colors. Hydrogen atoms have been omitted for clarity.

Arg310, and is near two polar residues, Gln71 and Tyr155, which may provide additional stabilizing interactions. The central phenyl ring B binds in a hydrophobic pocket formed by the aliphatic portion of the Gln72 sidechain, the phenyl ring of Tyr75 and the sidechain of Val45′. The pyridine (C ring) is bordered by residues Trp67, Ile68 and Val40′. The nitro group on the meta position of the pyridine is close to Arg193 to which it may form a hydrogen bond. This may explain why compound 1 is the most potent compound in the phenyl diacid series (Table 1). The overlay of docked compound 1 onto the crystal structure of W1807 (PDB entry 3AMV) is depicted in Fig. 5. Both compounds occupy a similar location inside the AMP allosteric site with their diacid groups interacting with arginines. However, the diacid functionality of compound 1 is almost perpendicular to that observed with W1807.

The predicted docking pose was confirmed by our X-ray crystal structure of RMGPb complexed with compound 1 [27,28]. The docked compound 1 occupies the same location inside the AMP allosteric site and maintains all major interactions. The rings A and B are overlaid with the diacid groups interacting with the positively charged arginines, Arg81, Arg309 and Arg310. The amide group next to ring B displays a different orientation, which causes the pyridines (ring C) to be poorly overlapped. However, the nitro group on ring C points to the same residue, Arg193, to form favorable interactions. The conformational difference in the amide and ring C region is accompanied by the substantial shift of sidechain orientation of Arg193 in the binding pockets. These will be the subject of discussion in a separate communication [28]. During the preparation of this manuscript, crystal structures of RMGPb complexed with similar diacid compounds were published by Kristiansen et al. [29]. Our proposed binding mode for compound 1 at the AMP allosteric site is similar to that of the compounds described therein.

3.3. Characterization of the binding pocket

Grid-based surfaces were calculated using the docking model to further characterize the binding pocket. Each grid was visualized as a series of iso-energetic surfaces, which describe the binding pocket by its polar (hydrogen bond donor and acceptor) and hydrophobic nature. The hydrophobic contour map is shown in Fig. 6. For clarity, the docked compound 1 is shown while the nearby residues in the binding pocket are omitted in the picture. In the hydrophobic contour map, the green area around compound 1 denotes the regions in the binding pocket, which favor interaction with a hydrophobic group on the ligand. For example, the green region near the pyridine (C ring) suggests that activity can be enhanced with appropriate hydrophobic substitutions on pyridine. This is in good agreement with the SAR in which compounds un-substituted on the C ring have the least activity while potency increases more than 10-fold with hydrophobic substitutions at the meta position (Table 1).

Similarly, there is a large area near the central phenyl ring B which is unfilled by compound 1 and for which SAR was unavailable. As was the case with the pyridine, this visually suggests that additional hydrophobic groups attached to the central phenyl B ring could fill this region and make favorable interactions with the residues which line this region of the binding pocket, thereby improving the binding, and thus, the potency.

3.4. Design

One possible modification was to fuse a hydrophobic ring onto the central phenyl ring B to access this putative hydrophobic region. Both saturated and unsaturated five and six member rings were considered. Energy evaluation was carried out by fully optimizing each virtual ligand within the flexible binding pocket. The interaction energy between each of the designed compounds and the enzyme was about 5–6 kcal/mol more favorable than that for the parent phenyl compound (Table 2). The fused ring moieties are nicely located between the aliphatic portion of the Gln72 sidechain, the phenyl ring of Tyr75 and the sidechain of Val45′, and make favorable interactions with the hydrophobic pocket. Based on synthetic considerations, compounds fused with an unsaturated six member ring (naphthyl compounds) were synthesized [27].

The potencies of naphthyl analogues are listed in Table 1 for comparison with the parent phenyl compounds. The

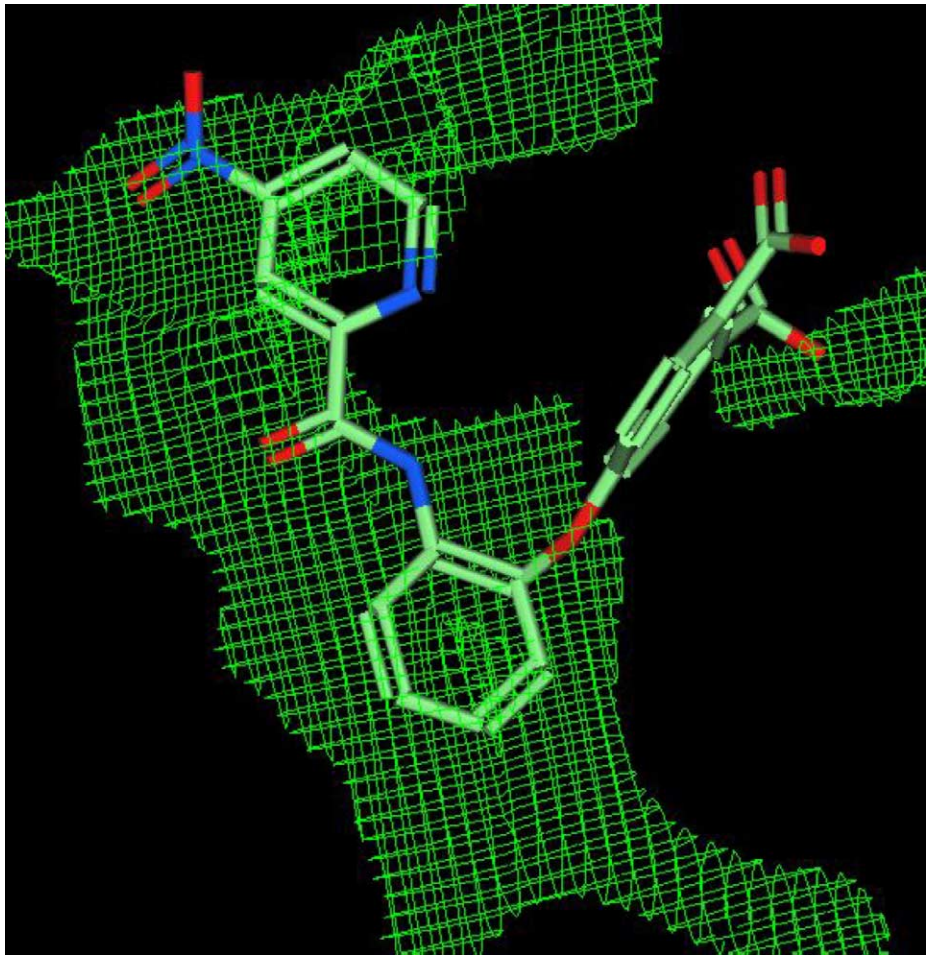

Fig. 6. Hydrophobic contour from grid-based calculations on docking model. Hydrophobic surface are shown in green grid. Compound 1 is shown in stick with carbons in green and non-carbon atoms in standard colors. Hydrogen atoms have been omitted for clarity.

Table 2
Energy calculation on the designed compounds

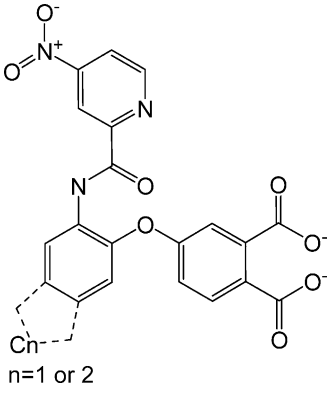

	Fused ring	Bond	Interaction energy (kcal/mol)
Compound 1	No	No	−112.6
Design 1	5	Saturated	−117.6
Design 2	5	Unsaturated	−118.6
Design 3	6	Saturated	−117.5
Design 4	6	Unsaturated	−118.6

potency is improved by 3–14-fold for HLGP and 7–19-fold for HMGP over the corresponding phenyl compounds. The enhancement in potency is consistent within the entire series and for both HLGP and HMGP. The naphthyl and phenyl series share a similar trend in potency change with different substitutions on the C ring: the un-substituted compounds are least active while the potency increases over 10-fold with hydrophobic substitutions on the meta position; the compounds with a nitro group are most potent. This indicates that the naphthyl and phenyl derivatives bind at the AMP allosteric site in a similar manner. The naphthyl series fills more space with the fused ring than the parent phenyl series, making more favorable interactions with surrounding residues and thereby increasing their potency.

4. Conclusion

In this paper, we describe modeling contributions directed towards the development of a new series of potent glycogen phosphorylase inhibitors. Due to the lack of suitable competition-based binding assays, superposition

was used to predict the potential binding site for lead compound 1. The overlay of compound 1 onto crystal structures of known inhibitors, which bind at different sites in GP, together with analysis of nearby residues at each respective site, correctly identified the AMP allosteric site as the binding site for compound 1. By using the crystal structure of RMGP (PDB entry 3AMV), possible docking modes of compound 1 were extensively explored by ICM calculations. A reasonable docking model was computationally determined and subsequently confirmed by X-ray crystallography. Further analysis of the binding pocket through the use of grid-based surface calculation revealed a large unfilled region near the central phenyl ring of compound 1. Fused ring analogues were designed with the goal of increasing hydrophobic bulk in this unfilled region to improve binding. After evaluation of energetics and ease of synthesis for this set of fused ring analogous, a series of naphthyl compounds were synthesized. As predicted, this exercise resulted in a new series of GP inhibitors with significantly improved potency.

References

[1] World Health Organization. Fact Sheet No.138, 2002.
[2] S.I. Talor, Deconstructing type 2 diabetes, Cell 97 (1999) 9–12.
[3] J.L. Treadway, P. Mendys, D.J. Hoover, Glycogen phosphorylase inhibitors for treatment of type 2 diabetes mellitus, Expert Opin. Investig. Drugs 10 (2001) 439–454.
[4] P. Jakobsen, J.M. Lundbeck, M. Kristiansen, J. Breinholt, H. Demuth, J. Pawlas, M.P. Torres Candela, B. Anderson, N. Westergaard, K. Lundgren, N. Asano, Iminosugars: potential inhibitors of liver glycogen phosphorylase, Bioorg. Med. Chem. 9 (2001) 733–744.
[5] W.H. Martin, D.J. Hoover, S.J. Armento, I.A. Stock, R.K. McPherson, D.E. Danley, R.W. Stevenson, E.J. Barrett, J.L. Treadway, Discovery of a human liver glycogen phosphorylase inhibitor that lowers blood glucose in vivo, Proc. Natl. Acad. Sci. USA 95 (1998) 1776–1781.
[6] L.N. Johnson, Glycogen phosphorylase: control by phosphorylation and allosteric effectors, FASEB J. 6 (1992) 2274–2282.
[7] V.L. Rath, M. Ammirati, P.K. LeMotte, K.F. Fennell, M.N. Mansour, D.E. Damley, T.R. Hynes, G.K. Schulte, D.J. Wasilko, J. Pandit, Activation of human liver glycogen phosphorylase by alteration of the secondary structure and packing of the catalytic core, Mol. Cell 6 (2000) 139–148.
[8] N.G. Oikonomakos, K.E. Tsitsanou, S.E. Zographos, V.T. Skamnaki, S. Goldmann, H. Bischoff, Allosteric inhibitor of glycogen phosphorylase a by the potential antidiabetic drug 3-isopropyl 4-(2-chlorophenyl)-1,4-dihydro-1-ethyl-2-methyl-pyridine-3,5,6-tricarboxylate, Protein Sci. 8 (1999) 1930–1945.
[9] S.E. Zographos, N.G. Oikonomakos, K.E. Tsitsanou, D.D. Leonidas, E.D. Chrysina, V.T. Skamnaki, H. Bischoff, S. Goldmann, K.A. Watson, L.N. Johnson, The structure of glycogen phosphorylase b with an alkyl-dihydropyridine-dicarboxylic acid compound, a novel and potent inhibitor, Structure 5 (1997) 1413–1425.
[10] N.G. Oikonomakos, J.B. Schnier, S.E. Zographos, V.T. Skamnaki, K.E. Tsitsanou, L.N. Johnson, Flavopiridol inhibits glycogen phosphorylase by binding at the inhibitor site, J. Biol. Chem. 275 (2000) 34566–34573.
[11] D.J. Hoover, S. Lefkowitz-Snow, J.L. Burgess-Henry, W.H. Martin, S.J. Armento, I.A. Stock, R.K. McPherson, P.E. Genereux, E.M. Gibbs, J.L. Treadway, Indole-2-carboxamide inhibitors of human liver glycogen phosphorylase, J. Med. Chem. 41 (1998) 2934–2938.
[12] N.G. Oikonomakos, V.T. Skamnaki, K.E. Tsitsanou, N.G. Gavalas, L.N. Johnson, A new allosteric site in glycogen phosphorylase b as a target for drug interactions, Structure 8 (2000) 575–584.
[13] V.L. Rath, M. Ammirati, D.E. Danley, J.L. Ekstrom, E.M. Gibbs, T.R. Hynes, A.M. Mathiowetz, R.K. McPherson, T.V. Olson, J.L. Treadway, D.J. Hoover, Human liver glycogen phosphorylase inhibitors bind at a new allosteric site, Chem. Biol. 7 (2000) 677–682.
[14] N.G. Oikonomakos, S.E. Zographos, V.T. Skamnaki, G. Archontis, The 1.76 Å resolution crystal structure of glycogen phosphorylase b complexed with glucose, and cp320626, a potential antidiabetic drug, Bioorg. Med. Chem. 10 (2002) 1313–1319.
[15] M.D. Miller, R.P. Sheridan, S.K. Kearsley, SQ: a program for rapidly producing pharmacophorically relevent molecular superpositions, J. Med. Chem. 42 (1999) 1505–1514.
[16] ICM-Pro 2.8 docking module, Molsoft LLC, San Diego, 2001.
[17] M.D. Miller, S.K. Kearley, D.J. Underwood, R.P. Sheridan, FLOG: a system to select 'quasi-flexible' ligands complementary to a receptor of known three-dimensional structure, J. Comput. Aided Mol. Des. 8 (1994) 153–174.
[18] C.M. Crippen, T.F. Havel, Distance Geometry and Molecular Conformation, Wiley, New York, 1988.
[19] T.A. Halgren, Merck molecular force field. I. Basis, form, scope, parameterization, and performance of MMFF94, J. Comput. Chem. 17 (1996) 490–519.
[20] T.A. Halgren, Merck molecular force field. II. MFF94 van der Waals and electrostatic parameters for intermolecular interactions, J. Comput. Chem. 17 (1996) 520–552.
[21] T.A. Halgren, Merck molecular force field. III. Molecular geometries and vibrational frequencies for MMFF94, J. Comput. Chem. 17 (1996) 553–586.
[22] T.A. Halgren, R.B. Nachbar, Merck molecular force field. IV. Conformational energies and geometries for MMFF94, J. Comput. Chem. 17 (1996) 587–615.
[23] T.A. Halgren, Merck molecular force field. V. Extension of MMFF94 using experimental data, additional computational data, and empirical rules, J. Comput. Chem. 17 (1996) 616–641.
[24] T.A. Halgren, Merck molecular force field. VI. MMFF94 option for energy minimization studies, J. Comput. Chem. 20 (1999) 720–729.
[25] T.A. Halgren, Merck molecular force field. VII. Characterization of MMFF94, MMFF94s, and other widely available force fields for conformational energies and for intermolecular-interaction energies and geometries, J. Comput. Chem. 20 (1999) 730–748.
[26] J.D. Thompson, D.G. Higgins, T.J. Gibson, CLUSTAL W: improving the sensitivity of progressive multiple sequence alignment through sequence weighting, position-specific gap penalties and weight matrix choice, Nucleic Acids Res. 22 (1994) 4673–4680.
[27] Z. Lu, J. Bohn, R. Bergeron, Q. Deng, K.P. Ellsworth, W.M. Geissler, G. Harris, P.E. McCann, B. McKeever, R.W. Myers, R. Saperstein, C.A. Willoughby, J. Yao, K.A. Chapman, New class of glycogen phosphorylase inhibitors, Bioorg. Med. Chem. Lett. 13 (2003) 4125–4128.
[28] B. McKeever, in preparation.
[29] M. Kristiansen, B. Anderson, L.F. Iversen, N. Westergaard, Identification, synthesis, and characterization of new glycogen phosphorylase inhibitors binding to the allosteric AMP site, J. Med. Chem. 47 (2004) 3537–3545.